Catalysis Letters Vol. 110, Nos. 1–2, August 2006 (© 2006)
DOI: 10.1007/s10562-006-0082-2

Catalyst deactivation and regeneration in low temperature ethanol steam reforming with $Rh/CeO_2–ZrO_2$ catalysts

Hyun-Seog Roh,[a,b] Alexandru Platon,[a] Yong Wang,[a,*] and David L. King[a]

[a]*Institute for Interfacial Catalysis, Pacific Northwest National Laboratory, PO Box 999, Richland, WA 99354, USA*
[b]*Korea Institute of Energy Research, 71-2 Jang-dong, Yuseong-gu, Daejeon 305-343, South Korea*

Received 4 December 2005; accepted 5 May 2006

$Rh/CeO_2–ZrO_2$ catalysts with various CeO_2/ZrO_2 ratios have been applied to H_2 production from ethanol steam reforming at low temperatures. The catalysts all deactivated with time on stream (TOS) at 350 °C. The addition of 0.5% K has a beneficial effect on catalyst stability, while 5% K has a negative effect on catalytic activity. The catalyst could be regenerated considerably even at ambient temperature and could recover its initial activity after regeneration above 200 °C with 1% O_2. The results are most consistent with catalyst deactivation due to carbonaceous deposition on the catalyst.

KEY WORDS: ethanol steam reforming; deactivation; regeneration; low temperature; $Rh/CeO_2–ZrO_2$.

1. Introduction

Hydrogen as a clean energy carrier has attracted significant interest. Commercially, methane steam reforming (MSR) is the primary method to produce hydrogen [1]. Due to transportability, liquid fuels such as methanol and ethanol are other candidates for hydrogen production via reforming. Methanol reforming has been considered extensively for the hydrogen production on account of its advantages of ready availability, absence of sulfur impurities, and ease of reforming at low temperatures [2–4]. However, methanol is toxic and may not be a renewable source. On the other hand, bio-ethanol is non-toxic and renewable, and can be produced by the fermentation of biomass-derived compounds. Ethanol produced from biomass is a nearly CO_2 neutral product. As a consequence, ethanol steam reforming is gaining increasing interest as a possible method for hydrogen production [5–12].

Compared to methanol steam reforming, ethanol steam reforming reaction pathways are more complicated due to the presence of a C–C bond. Ethanol steam reforming has been studied over transition metals and noble metals [8–17]. Rh catalysts have been favored for ethanol steam reforming because they show the greatest activity toward C–C bond cleavage [11,12]. Ethanol steam reforming has been more widely studied over the temperature range 600–700 °C, because high H_2 selectivity can be thermodynamically achieved at these high temperatures [18–21]. However, high temperature reforming favors co-production of CO, resulting in a loss of potential H_2 yield (due to the lack of favorable water gas shift equilibrium) and requiring significant down-stream CO minimization for PEM fuel cell applications. This adversely affects overall system efficiency due to heat losses and increases the capital cost for necessary hardware. As a result, low temperature ethanol reforming is an attractive alternative and has been studied by several researchers [8,22–25]. Raney Cu–Ni catalyst has recently been reported to exhibit stable activity for low temperature ethanol reforming (250–300 °C) [22]. However, hydrogen yield is lower from ethanol steam reforming with this catalyst. Oxidative steam reforming has also recently been studied to improve the low temperature ethanol steam reforming activity and hydrogen yield [8]. Introduction of oxygen as air has the disadvantage diluting the hydrogen product with N_2, which lowers fuel cell efficiency. The alternative, air separation, may be prohibitive economically. The challenge with low temperature ethanol steam reforming is to develop catalysts which are sufficiently active, and have high selectivity toward H_2 over CH_4. To do this requires kinetic control of the reforming process, since methane is the thermodynamically favored product. Recently, we have reported that $Rh/CeO_2–ZrO_2$ is selective to H_2 at low temperatures for ethanol steam reforming at 350 °C [26]. However, the $Rh/CeO_2–ZrO_2$ catalysts deactivate fairly rapidly.

The objective of this study was to elucidate the catalyst deactivation on $Rh/CeO_2–ZrO_2$ catalysts operating at low temperatures, and to develop facile methods of regeneration, if possible, at these same low temperatures.

*To whom correspondence should be addressed.
E-mail: yongwang@pnl.gov

2. Experimental

CeO_2–ZrO_2 supports with various Ce/Zr ratios were prepared by a co-precipitation method [27, 28]. Stoichiometric quantities of zirconyl nitrate solution (20 wt% ZrO_2 basis, MEL Chemicals) and Ce-nitrate (99.9%, Aldrich) were combined in distilled water. To this solution 15% ammonia solution was added dropwise at 80 °C to attain a pH of 10. The precipitate was digested at 80 °C for 3 days. After that, it was washed with distilled water several times and then air-dried for 48 h followed by drying at 110 °C for 6 h. Supported Rh catalysts (Rh = 2 wt%) were prepared by the incipient wetness method using a Rh nitrate solution. The catalysts were calcined at 500 °C for 6 h in air.

The BET surface areas were measured by nitrogen adsorption at −196 °C using a Micromeritics (ASAP-2400) surface area measurement apparatus. H_2 pulse chemisorption measurements were performed with an ASDI RXM-100 apparatus using the pulse equilibrium adsorption method. About 0.2 g of catalyst was placed in a quartz reactor. Before pulse chemisorption, the sample was reduced in 5% H_2/Ar at 350 °C for 1 h and evacuated at this temperature for 15 min before being cooled to −196 °C while evacuating. The total adsorption isotherm was measured volumetrically by consecutively expanding hydrogen trapped in a calibrated sample loop into the reactor containing the catalyst sample. The physisorption isotherm was measured similarly after a 10 min evacuation. Hydrogen chemisorption at −196 °C was determined as the difference between the total adsorption and physisorption isotherms. The catalyst sample was thereafter heated in 5% H_2/Ar at 350 °C for 10 min, evacuated at this temperature for 15 min and cooled to 20 °C under vacuum before being subjected to an additional H_2 chemisorption measurement at room temperature. 5% H_2/Ar and H_2 (ultra high purity, 99.999%) were used without further purification.

Temperature programmed oxidation (TPO) experiments were performed as follows. The ethanol steam reforming reaction was carried out in a 6 mm quartz micro-reactor under conditions similar to those used during activity experiments. The ethanol/water feed was discontinued at the chosen final reaction times and the reactor was rapidly removed from the furnace and allowed to cool to ambient temperature under a flow of He. The purge gas composition was subsequently changed to 2.4% O_2 in He with about 28 cm^3/min total flowrate. The system was allowed to equilibrate for about 1 h before the temperature was ramped at a rate of 10 °C/min up to 800 °C where it was held for 2 h. The effluent gas composition was monitored with an MKS PPT mass spectrometer system by recording the ion signal corresponding to $M/z = 44$ (CO_2). The amount of CO_2 generated was quantified from recorded peak areas using calibrations with CO_2 + He gas mixtures of known concentration.

Catalytic activity measurements were conducted at 1 atm with a fixed-bed micro-tubular quartz reactor having an inner diameter of 4 mm. The catalyst charge was 50 mg, and SiC was used as a catalyst diluent. A thermocouple was inserted into the catalyst bed to measure the reaction temperature. Prior to each catalytic measurement, the catalyst was reduced in H_2/N_2 (10% H_2 in vol.) at 350 °C for 1 h. Reactions were carried out at a steam to carbon ratio of 4 (H_2O/EtOH = 8). A mixture of ethanol and water was fed using a syringe pump and was vaporized at 250 °C upstream of the reactor [29]. The reformate was chilled, passed through an ice-trap to condense residual water and ethanol, and then flowed to the on-line gas chromatograph (GC) for analysis. An Agilent micro-GC with Molesieve 5A and PoraPlot Q columns was used in this study.

Following reaction, some catalyst samples were cooled to different temperatures and purged (30 min) under a flow of 50 cm^3/min N_2, and then subjected to *in-situ* regeneration in 1% O_2 while monitoring the CO_2 concentration in the effluent. The amount of CO_2 eluted was quantified by time integration of the CO_2 elution curve.

Ethanol conversion was calculated using a carbon balance on the gas phase products. N_2 was introduced as a reference gas to calculate the carbon balance. Traces of acetaldehyde, acetone and acetic acid were detected in the condensed liquid product but were not quantified within this study. The equations used in this study are as follows:

$$\text{EtOH conversion} = \text{Carbon}_{\text{out in gas phase}}/\text{Carbon}_{\text{in}}. \quad (1)$$

CO_2 selectivity was calculated using the carbon balance in the product gas stream. CO_2 selectivity is defined as follows.

$$CO_2 \text{ selectivity} = CO_2/(CH_4 + CO + CO_2 + 2C_2H_4). \quad (2)$$

CH_4, CO and C_2H_4 selectivities were also calculated using the carbon balance in the effluent. H_2 yield is defined as:

$$H_2 \text{ yield} = \text{moles of } H_2 \text{ produced/moles of EtOH fed.} \quad (3)$$

3. Results and discussion

3.1. Characterization

Table 1 summarizes the BET surface areas of the catalysts used in this study. The BET surface area of Rh/

Table 1
BET surface area of supported Rh catalysts (Rh = 2 wt%) used in this study

Catalyst	$Rh/Ce_{0.8}Zr_{0.2}O_2$	$Rh/Ce_{0.6}Zr_{0.4}O_2$	$Rh/Ce_{0.4}Zr_{0.6}O_2$	$Rh/Ce_{0.2}Zr_{0.8}O_2$
BET S.A. (m^2/g)	61	64	83	98

$Ce_{0.8}Zr_{0.2}O_2$ is 61 m^2/g. The BET surface area increases with increasing ZrO_2 content. The BET surface area of $Rh/Ce_{0.2}Zr_{0.8}O_2$ is 98 m^2/g.

It is known that accurate Rh dispersion is hard to estimate from H_2 chemisorption at ambient due to the hydrogen spillover from Rh to CeO_2–ZrO_2 [30,31]. Thus, H_2 chemisorption was carried out both at ambient temperature and at 77 K. It was assumed that the effect of the hydrogen spillover from Rh to CeO_2–ZrO_2 is minimal at 77 K. The resulting Rh dispersion values were calculated from the H_2 chemisorption results and are provided in table 2. At 77 K, all the catalysts showed approximately 25% dispersion. On the other hand, apparent Rh dispersion measured at ambient temperature increased with increasing CeO_2/ZrO_2 ratio. This indicates that the hydrogen spillover is occurring and correlates with CeO_2 content.

3.2. Reaction results

It is known that supports with redox properties enhance the reducibility of the supported metal and have desired properties in promoting the water gas shift (WGS) reaction. Among these supports, the Ce_{1-x}-Zr_xO_2 system is known to have high oxygen storage capacity (OSC), redox capability, and thermal stability [32–35]. As a result, the Ce_{1-x}-Zr_xO_2 system has been investigated for catalytic methane reforming [36–38]. Consistent with this, we have recently reported that Rh/CeO_2–ZrO_2 is selective to H_2 production over CH_4 formation at low temperatures with ethanol feedstock [26].

In this study, the CeO_2/ZrO_2 ratio was systematically varied to evaluate the effect of the CeO_2/ZrO_2 ratio on ethanol steam reforming. Table 3 summarizes the ethanol steam reforming testing results on these catalysts. It is clear that the $Rh/Ce_{0.8}Zr_{0.2}O_2$ catalyst exhibits the highest H_2 yield among the catalysts tested in this study. This catalyst shows the lowest CH_4 selectivity and the highest CO_2 selectivity. H_2 yield increase correlates with increasing CeO_2/ZrO_2 ratio. The trend of CO_2 selectivity is similar to that of H_2 yield, consistent with the WGS reaction being favored especially with supports having high CeO_2 content. In terms of stability, only the $Rh/Ce_{0.2}Zr_{0.8}O_2$ catalyst deactivated with time on stream under these test conditions, decreasing to 95% conversion at TOS of 10 h.

Based on the apparent deactivation of the $Rh/Ce_{0.2}Zr_{0.8}O_2$ catalyst, we decided to investigate activity maintenance with the series of Rh/Ce–Zr catalysts. To see the catalyst deactivation behavior within a short time period, the space velocity was increased to 243,000 cm^3/g_{cat}-h (table 4). Initially, all the catalysts showed 100% conversion, and all deactivated with time. The $Rh/Ce_{0.2}Zr_{0.8}O_2$ catalyst showed the most severe deactivation, with conversion declining to 14% by 7 h. The deactivation rate is strongly dependent upon the CeO_2/ZrO_2 ratio. The $Rh/Ce_{0.8}Zr_{0.2}O_2$ catalyst is more stable than other catalysts in ethanol steam reforming, which may be a result of increased oxygen storage capacity [27,38]. Figure 1 shows the ethylene selectivity increase with time over the Rh/CeO_2–ZrO_2 catalysts. The catalyst deactivation is closely correlated with ethylene formation. Because ethylene is considered a carbon precursor, it is likely that the catalyst deactivation is due to carbonaceous deposition.

To further evaluate the performance of the $Rh/Ce_{0.8}Zr_{0.2}O_2$ catalyst, experiments were conducted at temperatures as low as 350 °C at a high space velocity (480,000 $cm^3/h/g_{cat}$-h) in order to reduce the initial conversion below 100% (figure 2). Initially, ethanol conversion is around 70% and decreases to 6% after

Table 2
H_2 chemisorption results at 77 K and RT over supported Rh catalysts

Catalyst	Apparent Rh dispersion	
	77 K	293 K
$Rh/Ce_{0.8}Zr_{0.2}O_2$	25.3%	46.3%
$Rh/Ce_{0.6}Zr_{0.4}O_2$	26.8%	33.0%
$Rh/Ce_{0.4}Zr_{0.6}O_2$	21.0%	27.3%
$Rh/Ce_{0.2}Zr_{0.8}O_2$	25.8%	23.2%

Table 3
The effect of CeO_2/ZrO_2 ratio on EtOH steam reforming at 450 °C and 133,000 cm^3/g_{cat}-h space velocity

Catalyst	X_{EtOH} (%)	H_2/EtOH (m/m)	S_{CH_4} (%)	S_{CO} (%)	S_{CO_2} (%)
$Rh/Ce_{0.8}Zr_{0.2}O_2$	100	4.3	25	11	64
$Rh/Ce_{0.6}Zr_{0.4}O_2$	100	4.0	26	18	56
$Rh/Ce_{0.4}Zr_{0.6}O_2$	100	3.8	27	20	53
$Rh/Ce_{0.2}Zr_{0.8}O_2$	95	3.6	28	21	50

All the data were measured at the TOS of 10 h.

Table 4
The effect of CeO_2/ZrO_2 ratio on EtOH steam reforming at 450 °C and 243,000 cm^3/g_{cat}-h space velocity

Catalyst	X_{EtOH} (%)	H_2/EtOH (m/m)	S_{CH_4} (%)	S_{CO} (%)	S_{CO_2} (%)
$Rh/Ce_{0.8}Zr_{0.2}O_2$	61	2.6	19	43	37
$Rh/Ce_{0.6}Zr_{0.4}O_2$	57	2.2	23	47	30
$Rh/Ce_{0.4}Zr_{0.6}O_2$	46	1.8	24	36	39
$Rh/Ce_{0.2}Zr_{0.8}O_2$	14	0.6	22	20	53

All the data were measured at the TOS of 7 h.

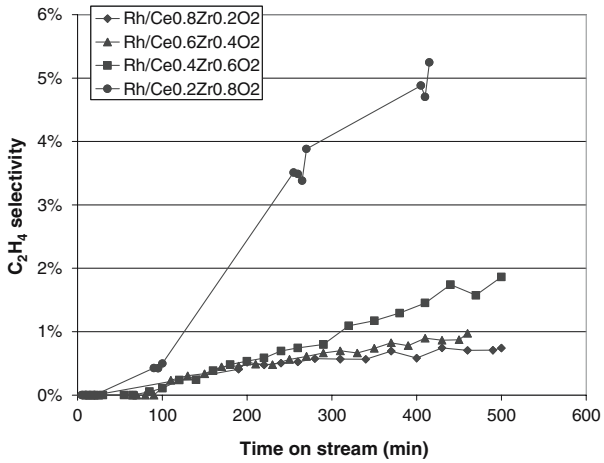

Figure 1. Ethylene selectivity with TOS over Rh/CeO_2–ZrO_2 catalysts at 450 °C and 243,000 cm^3/g_{cat}-h space velocity.

5 h. To suppress ethylene formation, potassium (as KOH) was added to the $Rh/Ce_{0.8}Zr_{0.2}O_2$ catalyst. Figure 2 shows the effect of K on ethanol conversion to gas phase products. It is obvious that the effect of K is significant on catalytic activity and stability. In the case of the 0.5% K-promoted catalyst, ethanol conversion is 12% at 350 °C (TOS = 300 min), which is twice that of the un-promoted catalyst. Initial ethanol conversion is around 47% with the 0.5% K-promoted catalyst, which is 20% lower than that of the un-promoted catalyst. Thus, it can be concluded that 0.5% K addition decreases the initial activity but increases the stability. On the other hand, the 5% K-promoted catalyst exhibits 2% conversion at TOS of 1 h, indicating that this high concentration has a negative effect on catalytic performance. Tests with a $Rh/Ce_{0.8}Zr_{0.2}O_2$ catalyst that was washed with a 2 wt% KOH solution and then rinsed with DI water prior to reduction indicated no significant change in catalyst behavior compared to the unpromoted catalyst.

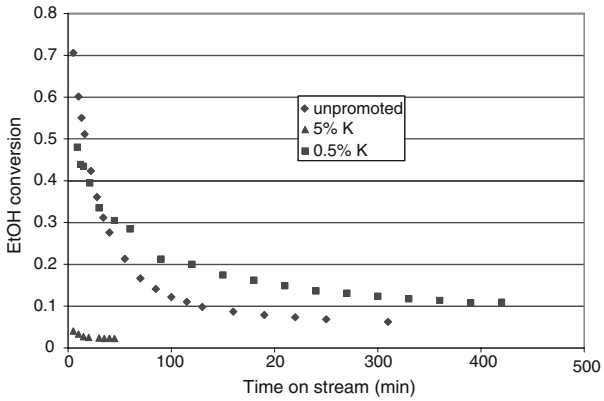

Figure 2. Effect of K on ethanol conversion to gas phase over the $Rh/Ce_{0.8}Zr_{0.2}O_2$ catalyst at 350 °C and 480,000 cm^3/g_{cat}-h space velocity.

To further understand the nature of the catalyst deactivation, the $Rh/Ce_{0.8}Zr_{0.2}O_2$ catalyst was regenerated with 1% O_2 at different temperatures (figure 3). It is surprising to see that the catalyst treated at ambient temperature shows sufficient regeneration to provide 25% ethanol conversion initially, which decreases to 6% after 100 min. For the catalyst regenerated at 150 °C, ethanol conversion is initially 45% and then drops to 7% after 100 min. In the case of the catalyst regenerated at above 200 °C, the initial conversion is around 65% and decreases to about 10% after 100 min. The results indicate that the catalyst can be at least partially regenerated with 1% O_2 at low temperature, with extent of regeneration increasing above 200 °C. During regeneration with 1% O_2, CO_2 was detected using GC-TCD detection at ambient temperature as well as above 200 °C (table 5). It is likely that Rh oxidizes carbonaceous deposit to produce CO_2. As a result of these experiments, it is concluded that the catalyst deactivation is due to carbonaceous deposition on catalyst.

To quantify the amount of carbonaceous material formed during the ethanol steam reforming reaction, TPO was combined with *in-situ* regeneration of the spent catalysts. Deposited carbonaceous build up was calculated from integrating the CO_2 quantities evolved. Figure 4 shows CO_2 evolved during TPO and residual

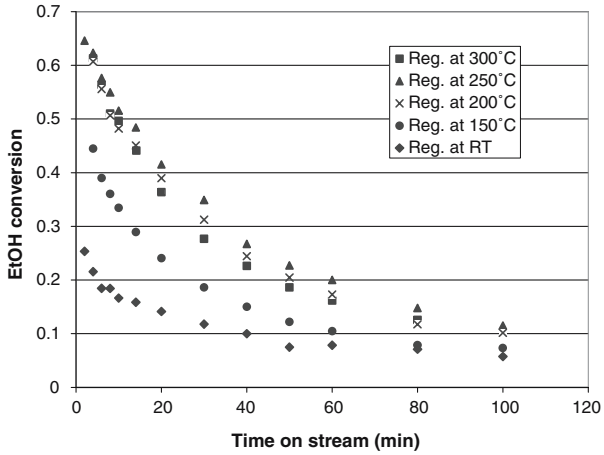

Figure 3. Effect of regeneration temperature on ethanol conversion at 350 °C and 480,000 cm^3/g_{cat}-h space velocity.

Table 5
Summary of TPO/*in-situ* regeneration results

Catalyst age (mol EtOH fed/g)	TOS (min)	X_{EtOH} (%)	CO_2 (mmol/g_{cat})	CO_2 peak (°C)
0.8	40	29	0.26	210
1.4	70	17	0.31	210
6.3[a]	310	6	1.02	–
6.3[b]	310	6	0.39	–

[a] *In-situ* regeneration at 200 °C.
[b] *In-situ* regeneration at 20 °C.

ethanol conversion as a function of catalyst age. Table 5 summarizes the TPO/*in-situ* regeneration results. It is obvious that carbonaceous material deposited on the catalyst increases with catalyst age, consistent with progressive catalyst deactivation. The maximum accumulation of carbonaceous intermediates measured was about 0.9 mmol/g_{cat} (figure 4). This represents a significant excess when compared with 0.2 mmol Rh/g_{cat} calculated for a 2 wt% Rh loading. When normalized to the BET surface area measured for this catalyst (table 1), a theoretical density of roughly 9 carbon atoms/nm^2 could be calculated. During the TPO experiments, a CO_2 peak appears at 210 °C, which is quite consistent with the regeneration results in figure 3. Deposited carbonaceous material on the catalyst from ethanol steam reforming could be eliminated above 200 °C with O_2. In the case of *in-situ* oxygen treatment at ambient temperature, CO_2 was immediately detected when 1% O_2 was introduced. Compared with the amount of CO_2 evolved during *in-situ* regeneration at 200 °C, approximately 38% carbonaceous material could be oxidized even at ambient temperature, which is in good agreement with the regeneration results in figure 3.

4. Conclusions

The Rh/CeO_2–ZrO_2 catalysts deactivate with time on stream in ethanol steam reforming, when operating at high space velocities and low temperatures. In the case of the $Rh/Ce_{0.8}Zr_{0.2}O_2$ catalyst, the deactivation rate is slower. Addition of 0.5% K (as KOH) has a beneficial effect on catalyst stability, while 5% K has a negative effect on catalytic activity. The deactivated catalyst can be regenerated to some extent even at ambient temperature and is regenerated completely above 200 °C with 1% O_2. The catalyst deactivation appears to be due to carbonaceous deposition on catalyst.

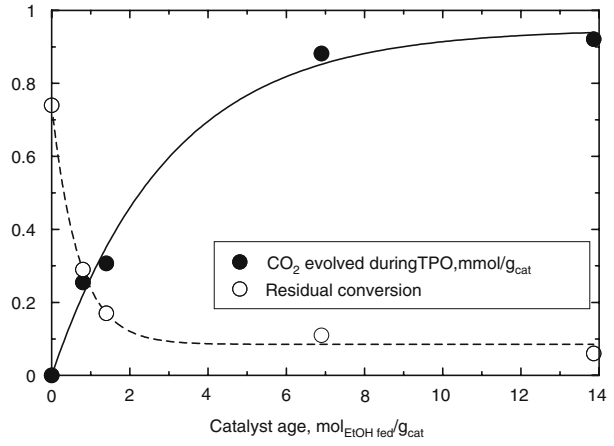

Figure 4. Measured CO_2 evolved during TPO and corresponding residual conversion following steam reforming of ethanol at 350 °C.

Acknowledgments

This work was supported by Department of Energy's Office of Hydrogen, Fuel Cells, and Infrastructure Technologies. Most of work was performed in the Environmental Molecular Science Laboratory, a national scientific user facility sponsored by the U.S. Department of Energy's Office of Biological and Environmental Research and located at Pacific Northwest National Laboratory in Richland, WA.

References

[1] J.R. Rostrup-Nielsen, in: *Catalysis, Science and Technology*, Vol. 5, eds. J.R. Anderson and M. Boudart (Springer, Berlin, 1984) p. 1.
[2] C. Cao, G. Xia, J. Holladay, E. Jones and Y. Wang, Appl. Catal. A 262 (2004) 19.
[3] C.S. Song, Catal. Today 77 (2002) 17.
[4] S. Velu and K. Suzuki, Topics Catal. 22 (2003) 235.
[5] G.W. Huber, J.W. Shabaker and J.A. Dumesic, Science 300 (2003) 2075.
[6] R.D. Cortright, R.R. Davda and J.A. Dumesic, Nature 418 (2002) 964.
[7] G.A. Deluga, J.R. Salge, L.D. Schmidt and X.E. Verykios, Science 303 (2004) 993.
[8] J. Kugai, S. Velu and C. Song, Catal. Lett. 101 (2005) 255.
[9] J. Llorca, P.R. de la Piscina, J.A. Dalmon, J. Sales and N. Homs, Appl.Catal. B 43 (2003) 355.
[10] S. Velu, N. Satoh, C.S. Gopinath and K. Suzuki, Catal. Lett. 82 (2002) 145.
[11] D.K. Liguras, D.I. Kondarides and X.E. Verykios, Appl. Catal. B 43 (2003) 345.
[12] J.P. Breen, R. Burch and H.M. Coleman, Appl. Catal. B 39 (2002) 65.
[13] A.N. Fatsikostas, D.I. Kondarides and X.E. Verykios, Catal. Today 75 (2002) 145.
[14] D. Srinivas, C.V.V. Satyanarayana, H.S. Potdar and P. Ratnasamy, Appl. Catal. A 246 (2003) 323.
[15] A. Haryanto, S. Fernando, N. Murali and S. Adhikari, Energy Fuels 19 (2005) 2098.
[16] A.N. Fatsikostas and X.E. Verykios, J. Catal. 225 (2004) 439.
[17] F. Haga, T. Nakajima, H. Miya and S. Mishima, Catal. Lett. 48 (1997) 223.
[18] K. Vasudeva, N. Mitra, P. Umasankar and S.C. Dhingra, Int. J. Hyrogen Energy 21 (1996) 13.
[19] I. Fishtik, A. Alexander, R. Datta and D. Geana, Int. J. Hyrogen Energy 25 (2000) 31.
[20] S. Freni, G. Maggio and S. Cavallaro, J. Power Sources 62 (1996) 67.
[21] P. Tsiakaras and A. Demin, J. Power Sources 102 (2001) 210.
[22] D.A. Morgenstern and J.P. Fornango, Energy Fuels 19 (2005) 1708.
[23] W. Wang, Z. Wang, Y. Ding, J. Xi and G. Lu, Catal. Lett. 81 (2002) 63.
[24] C. Diagne, H. Idriss and A. Kiennemann, Catal. Commun. 3 (2002) 565.
[25] C. Diagne, H. Idriss, K. Pearson, M.A. Gomez-Garcia, A. Kiennemann, C. R. Chimie. 7 (2004) 617.
[26] H.-S. Roh, Y. Wang, D.L. King, A. Platon and Y.-H. Chin, Catal. Lett. 108 (2006) 15.
[27] H.S. Potdar, H.-S. Roh, K.-W. Jun, M. Ji and Z.-W. Liu, Catal. Lett. 84 (2002) 95.
[28] H.-S. Roh, H.S. Potdar, K.-W. Jun, J.-W. Kim and Y.-S. Oh, Appl. Catal. A 276 (2004) 231.

[29] D.R. Palo, J.D. Holladay, R.T. Rozmiarek, C.E. Guzman-Leong, Y. Wang, J. Hu, Y.-H. Chin, R.A. Dagle and E.G. Baker, J. Power Sources 108 (2002) 28.
[30] C. Dall'Agnol, A. Gervasini, F. Morazzoni, F. Pinna, G. Strukul and L. Zanderighi, J. Catal. 96 (1985) 106.
[31] W.K. Jozwiak, React. Kinet. Catal. Lett. 30 (1986) 345.
[32] A. Trovarelli, Catal. Rev.-Sci. Eng. 38 (1996) 439.
[33] J. Kaspar, P. Fornasiero and M. Graziani, Catal. Today 50 (1999) 285.
[34] S. Rossignol, F. Gerard and D. Duprez, J. Mater. Chem. 9 (1999) 1615.
[35] M. Thammachart, V. Meeyoo, T. Risksomboon and S. Osuwan, Catal. Today 68 (2001) 53.
[36] H.-S. Roh, K.-W. Jun, W.-S. Dong, S.-E. Park and Y.-S. Baek, Catal. Lett. 74 (2001) 31.
[37] H.-S. Roh, K.-W. Jun, W.-S. Dong, J.-S. Chang, S.-E. Park and Y.-I. Joe, J. Mol. Catal. A 181 (2002) 137.
[38] H.-S. Roh, H.S. Potdar and K.-W. Jun, Catal. Today 93–95 (2004) 39.